

This article was downloaded by:

On: 22 January 2011

Access details: *Access Details: Free Access*

Publisher *Taylor & Francis*

Informa Ltd Registered in England and Wales Registered Number: 1072954 Registered office: Mortimer House, 37-41 Mortimer Street, London W1T 3JH, UK



The Journal of Adhesion

Publication details, including instructions for authors and subscription information:

<http://www.informaworld.com/smpp/title~content=t713453635>

Fiber-Matrix Interfacial Adhesion Improvement in Carbon Fiber-Bisphenol-A Polycarbonate Composites by Polymer Grafting

Venkat K. Raghavendran^a; Lawrence T. Drzal^a

^a Composite Materials and Structures Center, Michigan State University, East Lansing, Michigan, USA

Online publication date: 08 September 2010

To cite this Article Raghavendran, Venkat K. and Drzal, Lawrence T.(2010) 'Fiber-Matrix Interfacial Adhesion Improvement in Carbon Fiber-Bisphenol-A Polycarbonate Composites by Polymer Grafting', *The Journal of Adhesion*, 78: 10, 895 – 922

To link to this Article: DOI: 10.1080/00218460214096

URL: <http://dx.doi.org/10.1080/00218460214096>

PLEASE SCROLL DOWN FOR ARTICLE

Full terms and conditions of use: <http://www.informaworld.com/terms-and-conditions-of-access.pdf>

This article may be used for research, teaching and private study purposes. Any substantial or systematic reproduction, re-distribution, re-selling, loan or sub-licensing, systematic supply or distribution in any form to anyone is expressly forbidden.

The publisher does not give any warranty express or implied or make any representation that the contents will be complete or accurate or up to date. The accuracy of any instructions, formulae and drug doses should be independently verified with primary sources. The publisher shall not be liable for any loss, actions, claims, proceedings, demand or costs or damages whatsoever or howsoever caused arising directly or indirectly in connection with or arising out of the use of this material.



FIBER-MATRIX INTERFACIAL ADHESION IMPROVEMENT IN CARBON FIBER-BISPHENOL-A POLYCARBONATE COMPOSITES BY POLYMER GRAFTING

Venkat K. Raghavendran

Lawrence T. Drzal

Composite Materials and Structures Center,
Michigan State University, East Lansing, Michigan, USA

Fiber-matrix interfacial adhesion in thermoplastic composites is generally poor due to the lack of formation of strong covalent and/or ionic bonds between the generally inert thermoplastic resins and the surface of the reinforcing fiber. Adhesion can be improved by forming covalent linkages between the fiber and the matrix by grafting a polymer of appropriate compatibility, molecular weight, and sufficient density onto the surface of the fiber. We have grafted low molecular weight polycarbonate and polymethyl methacrylates onto the surface of carbon fibers and measured an improvement in the level of adhesion ranging from 25% to 100% over the ungrafted composites. It was also observed that the level of improvement in adhesion appears to be independent of the molecular weight of the grafted polymer. Examination of the fracture surface of these composites reveals that the failure is cohesive in the matrix for the polymer grafted fiber composites, while it is adhesive for the ungrafted composites.

Keywords: Grafting; Fiber-matrix adhesion; Polycarbonate; Polymethyl methacrylate; Microindentation test; Transverse tensile test; Scanning electron microscopy

Received 10 February 2001; in final form 29 April 2002.

This is one of a collection of papers honoring Hatsuo (Ken) Ishida, the recipient in February 2001 of *The Adhesion Society Award for Excellence in Adhesion Science*, Sponsored by 3M.

The authors wish to thank the Office of Naval Research, Grant No. N00014-93-1-0186, and the State of Michigan Research Excellence Fund for the financial support for this work.

Address correspondence to Lawrence T. Drzal, Composite Materials and Structures Center, 2100 Engineering Building, Michigan State University, East Lansing, MI 48824-1326, USA. E-mail: drzal@egr.msu.edu

INTRODUCTION

It is well known that carbon fibers have excellent mechanical properties. Their high structural strength and modulus makes them desirable material in a large number of applications as the reinforcing medium. However, due to their high cost of production, composite materials containing carbon fibers have been mostly restricted to aerospace applications, where cost is secondary to performance. Now, however, with the reduction in their prices because of the availability of the fibers in larger tows, they are poised to play a major role in increasing the use of composites in high-volume markets such as transportation and infrastructure. Since ease of processing, good impact strength, and recyclability are of major importance, graphite-fiber-reinforced polymer matrix composites need to be fabricated with thermoplastic matrices. Thermoplastic matrices have desirable properties of good impact strength, ease of processing, and recyclability but are handicapped by the low level of adhesion they exhibit with carbon fibers. This low level of adhesion may be due to a lack of formation of strong covalent bonds, insufficient wetting, and interlocking with the fiber surface.

In one of our studies on interfacial adhesion [1, 23] we found that increasing the level of surface oxygen and the surface roughness did not result in any discernable improvement in the interfacial adhesion in these systems, indicating that van der Waals interactions either alone or in combination with mechanical interlocking are insufficient to ensure high levels of adhesion.

However, we have seen an improvement in the interfacial adhesion with increasing molecular weight of the polycarbonate matrix and interphase with higher processing temperature [2]. The improvement in the level of adhesion with higher molecular weight was attributed to the formation of a beneficial interphase in which the polycarbonate molecules experienced stronger adsorption and better fiber wetting at higher processing temperatures. However, increasing the molecular weight also results in a higher viscosity and requires increasing the processing temperature to assist with wetting and impregnation of the fiber tows, at the risk of polymer degradation. Further, it was also shown that the use of polydisperse matrices or low molecular weight additives to improve the processability results in entropically driven segregation of low molecular weight polymer to the fiber-matrix interface, resulting in lowering of the level of adhesion. The ability to maintain the concentration of high molecular weight polymer at the interphase and prevent it from being displaced by lower molecular weight polymer appears to be an important factor for achieving improvement of adhesion of thermoplastics to carbon fibers.

Retention of the high molecular weight species at the fiber surface can be accomplished in two ways: thermodynamically, by increasing the enthalpic contribution, or physically, by immobilizing higher molecular weight chains at the interface by either tethering them to the surface or crosslinking them in the interphase around the fiber surface. In our previous studies [1, 23] an attempt to increase the enthalpic contribution by increasing the amount of polar and hydrogen bonding groups on the surface showed that increasing the surface functionality alone had a minimal effect on fiber-matrix adhesion. Crosslinking the high molecular weight chains at the interface in order to immobilize them is not possible for all types of polymers. Further, crosslinking the chains constrains their mobility as well as their interdiffusion potential and reduces their flexibility and, therefore, the toughness of the crosslinked interphase, which can lead to an increase in brittle failure of the interface region. Tethering the polymer chains by their ends at the interface, however, would provide sufficient mobility for the chains to deform under load and therefore retain polymer and interphase toughness.

Tethering polymer chains by their end results in three major conformations, namely mushrooms, pancakes, and brushes [3, 4]. These conformations of the tethered chain are very different from the conformations exhibited by ungrafted chains. These differences in conformation can result in very different properties for the grafted chains with regards to their ability to entangle with the bulk chains.

A large body of research has been published on the effects of areal density of surface grafts, the conformation of the grafted chains, the fracture rate, etc. on the interfacial adhesion in grafted fiber composites. Excellent reviews of various theories and experimental work on grafted polymer chains are available [5, 10]. However, there is a limited amount of experimental work available in the literature on the effect of polymer chain length on interfacial adhesion of end-grafted composites. Dibenedetto et al. [6] found a decrease in the interfacial adhesion with increasing molecular weight of the grafted chain in polycarbonate-grafted glass fiber composites. However, annealing the grafted composite for a longer time resulted in improvement in the interfacial adhesion of the higher molecular weight grafted composites. The final level of adhesion becomes independent of the molecular weight. Chou and Penn [7] have shown that in aramid-fiber-reinforced epoxy composites, grafting polyamides on the fiber surface resulted in an improvement in adhesion. As the grafted oligomer length was increased from 2 to 6 times, they found that the interfacial adhesion increased from 20% to 60%. Kramer et al. [8] have studied the effect of the molecular weight of a grafted layer of deuterated polystyrene on

the interfacial adhesion between an epoxy and polystyrene. It was seen in their study that, at a lower degree of polymerization, there was no improvement in the fracture toughness of the interface, while at higher degree of polymerization the fracture toughness, G_c , was seen to be independent of the chain length. They also observed that above a critical areal density the grafted polymer chains at the interface fail by chain scission, while below this critical areal density the failure occurs by chain pull out, as shown in Figure 1. Their observations are consistent with the theory of cohesive zone models and crack growth proposed by Xu et al. [9].

The fracture mechanism map predicts that the interface modified with short grafted chains will fail by pull out of the grafted chains from the thermoplastic matrix when a stress, σ_{pullout} , is reached (Figure 2).

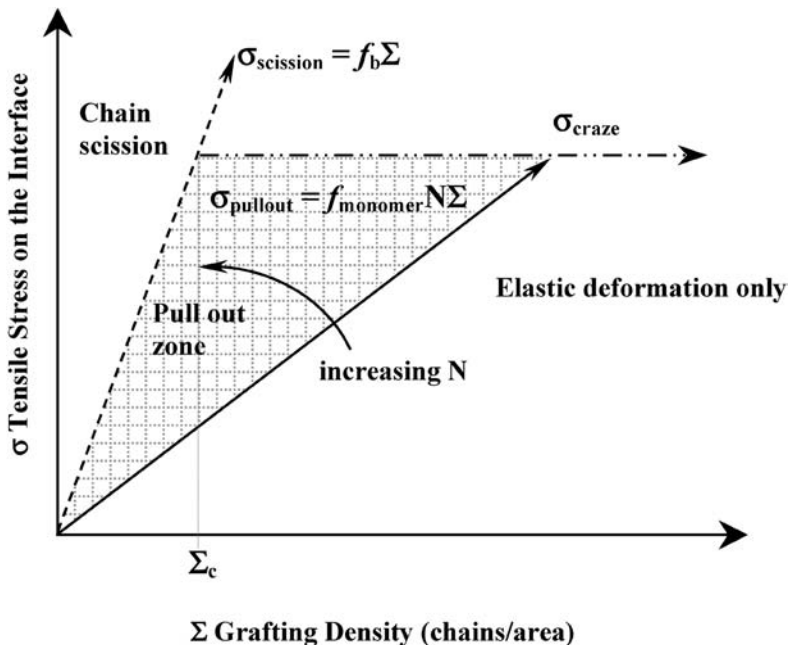


FIGURE 1 Tensile stress on interface, σ , plotted *versus* the grafting density, Σ , of the chains anchored by one end to the interface. The craze widening stress on the interface is shown as a dot-dashed line. The stress required to break the backbone bonds of the grafted chain is shown with a dashed line. The stress on the interface for the pull out of grafted chain is shown with a solid line [9, 10].

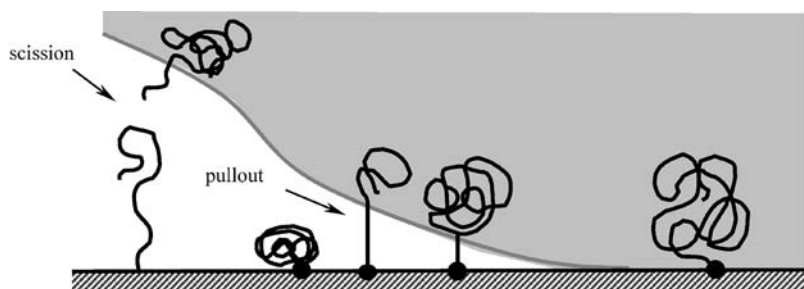


FIGURE 2 Schematic diagram of the chain pull out and scission process that takes place as the crack grows along the interface. For low molecular weight chains, as the crack advances each connector is stretched to its maximum length and gets pulled out; it then collapses on the surface [10]. For the high molecular weight chains, the stress can exceed the strength of the bond between the backbone molecules, resulting in chain scission [9].

This stress depends linearly on the degree of polymerization, N , the areal density of the grafted chain, Σ , and the static friction coefficient, f_{monomer} , between a monomeric segment of the grafted chain and the surrounding matrix. As N increases, additional stress will be required to fracture the interface and eventually the stress exceeds the fracture strength (*i.e.*, molecular bond strength) of the grafted chain backbone. At low grafting densities, $\Sigma < \Sigma_C$, the interface will fail when there is sufficient force, f_b , on the backbone of the grafted chains to cause chain scission. Interface failure will occur when the interfacial stress exceeds $\sigma_{\text{scission}} = f_b \Sigma$. As Σ increases, the areal density of the entanglements between the grafted brushes and matrix will provide effective stress transfer across the interface to cause large-scale plastic deformation. The transition from σ_{scission} to a stress-causing large-scale plastic deformation or crazing, σ_{craze} , occurs when the strength of the grafted interface is higher than the yield strength of the grafted chains. As the stress is increased further, fracture of the samples with $\Sigma > \Sigma_C$ will occur by craze failure *via* pullout of the grafted chains or by scission of chains in a fibrillar structure [10].

The intent of the research reported in this paper is to investigate the effect of grafting polymers to fiber surfaces and to determine the effect of the grafts on fiber-matrix adhesion in composite materials. For this study, we grafted bisphenol-A polycarbonate and polymethyl methacrylate on to the surface of polyacrylonitrile-based carbon fibers *via* anionic polymerization. The reaction of the fiber surface with butyl lithium in the presence of N, N, N', N' , tetra methyl ethylene diamine

and 18 crown-6 crown ether was found to be the most effective method to produce highly active metallized aromatic groups capable of initiating anionic polymerization. The grafting of polycarbonate on to the surface proceeded *via* a ring opening polymerization of cyclic oligocarbonates, while Polymethyl Methacrylate (PMMA) was formed through the consumption of Methyl Methacrylate (MMA) monomer, as shown in Figure 3. The degree of polymerization of polycarbonate was found to be low, while that of polymethyl methacrylate was high. A detailed description of the grafting process and the amount and molecular weight of the polymer grafted onto the surface of the carbon fiber is given in Raghavendran and Drzal [11, 23]. In the present study, due to the constraints of the reaction we were unable to produce grafted polycarbonate of high molecular weight. The use of Tetrahydrofuran (THF) as the solvent in the grafting reaction is probably the reason for the formation of lower molecular weight grafted Bisphenol-A Polycarbonate (BPA-PC) chains. Since THF is a poor solvent for BPA-PC, it precipitates out of the system once it reaches a particular degree of polymerization. The BPA-PC formed has a molecular weight of around 5000 Daltons, which is one-sixth the molecular weight of the bulk matrix used in the study. We were, however, constrained to use THF, as most of the good solvents for BPA-PC such as CH_2Cl_2 , dichlorobenzene, and CHCl_3 were susceptible to attack by butyl lithium. Therefore, to study the effect of grafting a polymer of much higher molecular weight than the bulk, we had to use a polymer that could blend with BPA-PC and have similar mechanical properties. PMMA was found to be an ideal choice. With the solubility parameters of BPA-PC being $19.3 (\text{J}/\text{m}^3)^{1/2}$ [12] and PMMA ranging from 18.8 to $20.3 (\text{J}/\text{m}^3)^{1/2}$ [12, 13], a large body of published research [14–17] has shown that the interaction between BPA-PC and PMMA is favorable enough to form miscible blends when both components have molecular weights typical of useful polymers [14] (M_w of 25 K to 35 K Daltons for BPA-PC and 100 K to 200 K Daltons for PMMA). The PMMA grafted on to the IM7 series fibers has six times the molecular weight of the BPA-PC used as the bulk matrix in the present study. Blends of BPA-PC and PMMA have been used for gas separation membranes [18], stabilization of PMMA from photodegradation [19], and enhancement of toughness [20]. Homogeneous blends of PC and PMMA, which are transparent and have a single glass transition temperature, T_g , lying in between their individual T_g , can be formed when cast from THF at elevated temperature (47°C) [21]. However, these blends are not thermodynamically stable and tend to phase separate between 150°C and 220°C , again forming a homogeneous blend when processed above 220°C [22].

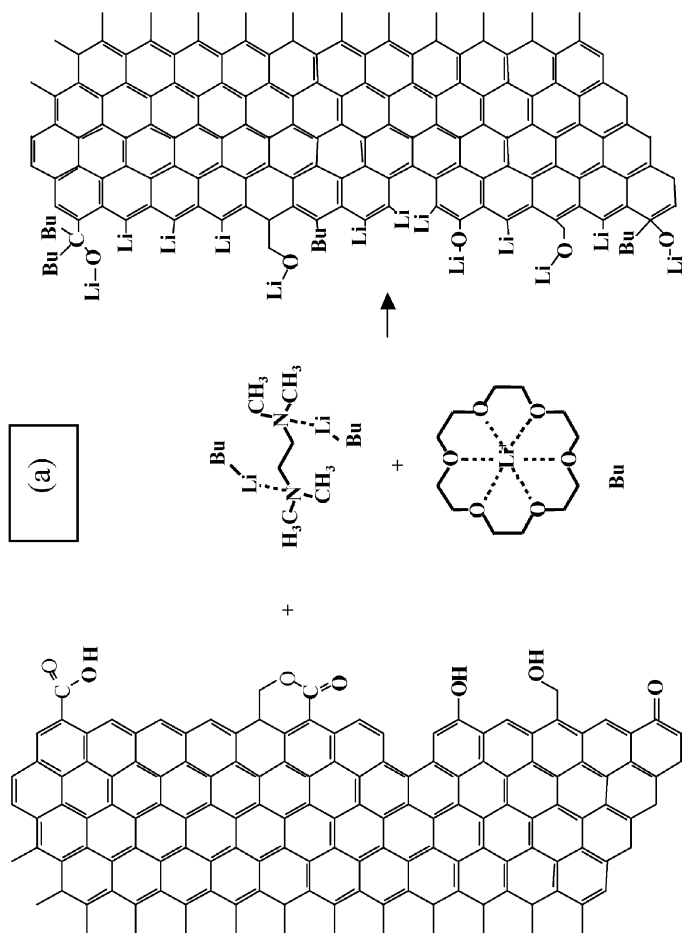


FIGURE 3 (a) Schematic diagram of metalation of the carbon fiber surface by butyl lithium in the presence of a chelating agent such as TMEDA, and a cation complexation agent such as 18 crown 6. (b) Schematic diagram of the polymerization of cyclic BPA-PC oligomers and MMA on a metallized carbon fiber surface. (*Continued.*)

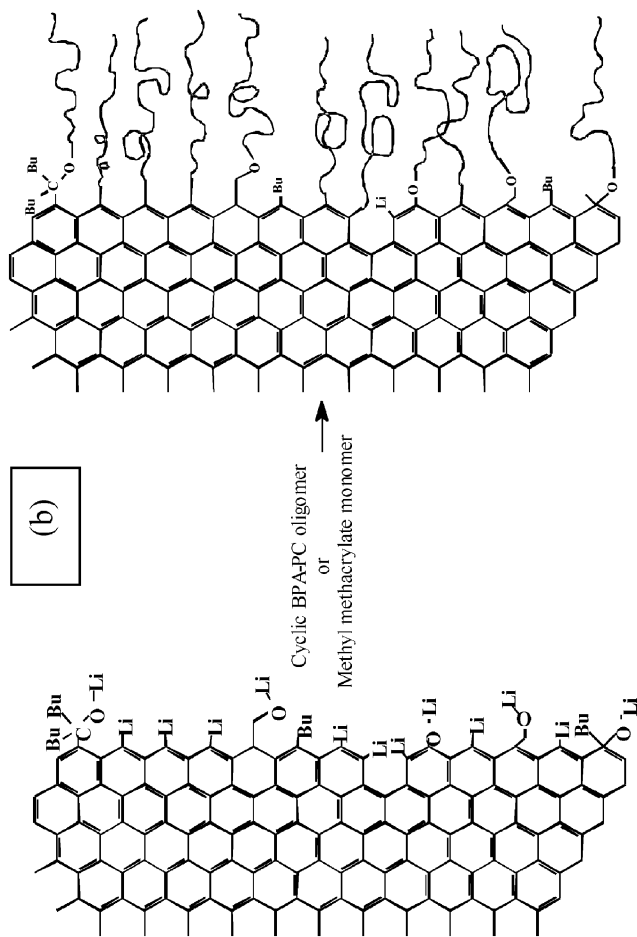


FIGURE 3 (Continued.)

EXPERIMENTAL

Materials and Processing Method

For preparing the polymer-grafted fiber composites, two sets of the polyacrylonitrile-based, intermediate modulus IM7 series carbon fiber from Hexcel Corporation (Salt Lake City, Utah) were used. One set contained fibers with different degrees of fiber surface treatment ranging from 20% to 400% of the nominal commercial treatment levels. The other set contained oxidized fibers that had had their surfaces passivated in hydrogen. The oxidative surface treatment changed the surface oxygen content of the carbon fibers. The oxygen content of the carbon fiber surface increased from 4% to 22% by changing the degree of surface treatment from 0% to 400% of nominal commercial surface treatment levels. The oxidative surface treatment also causes an increase in surface roughness by creating pores and fissures in the surface by removing carbon from the regions between the graphite crystallites. To decouple the effects of surface roughness and the surface oxides on the interfacial adhesion, the oxidized fiber surface was passivated *via* hydrogenation at elevated temperature. Thermal hydrogenation removes the oxides on the surface without significantly altering the surface topography. A detailed description of the oxidation and thermal hydrogen passivation of the fibers used in this study is given in Raghavendran and Drzal [23]. The oxidized fiber tows were grafted with either BPA-PC or PMMA by converting the graphitic edge surface groups on the carbon fiber surface into anions and initiating the polymerization described earlier. The hydrogenated fibers were also grafted with PMMA in a similar manner. The BPA-PC grafted on to the carbon fiber surface were low molecular weight chains with a molecular weight of around 5000 Daltons, while the PMMA grafted on the surface were high molecular weight, ranging from 55,000 Daltons to 225,000 Daltons.

The polymer used as the bulk matrix was Bisphenol-A polycarbonate. The BPA-PC was a high molecular weight, low melt flow index grade polycarbonate having an average molecular weight of 31,000 Daltons. The polycarbonate was supplied by GE Plastics, Inc., (Mt. Vernon, Indiana) without any additives or stabilizers. The polymer-grafted fibers, after thorough washing and extraction of ungrafted bulk polymerized material by Soxhlet extraction in a good solvent, were then dipped for 60 minutes in a 10% w/w solution of the high molecular weight BPA-PC in chloroform to swell the grafted chains and allow bulk PC to reptate and entangle with the swollen grafted polymer layer. The fiber bundle was then carefully spread into a thin

tape, one inch (2.5 cm) wide, and allowed to dry in air and later in a vacuum oven at 70°C to remove the solvent completely. The carbon-reinforced, thermoplastic polycarbonate composites were fabricated from the amorphous BPA-PC resin and the polymer-grafted IM7 fibers by compression molding. The composite samples fabricated for microindentation tests were processed according to the hot press fabrication technique described in previous research [1, 28, 29].

Prior to the fabrication of the composite specimens, preform sheets, one-third of the final thickness, were prepared by hot pressing of the oven-dried polycarbonate powder between acetone-cleaned, 30 μm thick, optically smooth Kapton[®] polyimide sheets, with the thickness controlled by a surrounding stainless steel dam. The preform sheets were produced at 250°C and a pressure of 3.45 MPa, with a residence time of 5 minutes at the consolidation temperature. The time and temperature for the preliminary step were kept as low as possible to minimize thermal degradation, as these preform sheets would have to undergo reconsolidation at a higher temperature. The thin polyimide sheets were used to avoid the use of release agents which can cause surface contamination. The polyimide sheets are nonbonding and can easily be peeled off the polycarbonate sheets without deforming them. Further, thin films of polycarbonate 5 to 15 μm thick were cast from a solution of polycarbonate in methylene chloride for interleaving and lamination of the fiber bundles during the composite fabrication.

For the fabrication of composite specimens, two 15 cm × 10 cm polycarbonate preform sheets, thoroughly cleaned with isopropyl alcohol, were used. One preform sheet was placed on a smooth 30 μm thick Kapton[®] polyimide sheet, and two 2 mm thick × 2 mm wide spacer strips were placed on the two edges lengthwise to bear the load during the initial part of the consolidation cycle. The preform sheet was then draped with the polymer-grafted carbon fiber tow followed by the solution-cast polycarbonate film. Another 3 alternating layers of fiber tow and polycarbonate film were then stacked on top of each other and, finally, the upper preform sheet was placed on the top of this layered assembly. This fiber matrix assembly was surrounded by a 3 mm thick stainless steel dam. A smooth Kapton[®] polyimide sheet was then placed over the assembly and the entire assembly was vacuum bagged for the consolidation. The composite fabrication of the 15 cm × 10 cm polycarbonate preform sheets was done using a multi-step consolidation cycle on a programmable, smart Tetrahedron[®] press. In the initial step a very small load of 0.3 tons (producing a pressure of ~0.17 Mpa) was placed on the platens to ensure intimate contact between the precomposite assembly and the platens for obtaining uniform heating of the specimen. The temperature was

ramped at a rate of 5°C/minute upto 125°C, and the assembly was allowed to soak at this temperature for half an hour to remove any traces of moisture on the fiber surface and the polycarbonate. Following the 125°C soak, the temperature was ramped upto 275°C at a rate of 5°C/minute. Upon reaching the consolidation temperature, a load pressure of 6.9 MPa was applied and maintained throughout the pressing cycle. The specimen was consolidated for 15 minutes and then cooled at approximately 1°C/second to 30°C. The composite specimens were then cut into 1 cm × 1 cm samples and fixed with polyester resin in a sample holder, with the fibers lying normal to sample surface, and polished according to standard metallographic technique to optical smoothness.

A second set of specimens was made under the same processing condition using the prepregged fiber bundle to produce high volume fraction, aligned-fiber composites for transverse tensile testing. However, due to constraints of the reaction setup, only a small amount of fibers could be grafted per batch [11], and hence there was not a sufficient number of high fiber volume fraction composites to do a standardized transverse tensile test on them. The composite specimens produced were only 2 mm in thickness. To test the composite specimens without damaging them, and also to produce a uniform stress field across them, the composites were sintered onto a 0.5 mm thick polycarbonate sheet at 200°C at a pressure of 10 MPa. Similar test specimens were also made using ungrafted fiber bundles for comparing the transverse tensile properties of these composites. The test specimens were then cut into 50 mm × 12.5 mm pieces within the composite part lying on the surface of the polycarbonate sheet in the middle of the specimen measuring 12.5 mm × 12.5 mm.

Composite Test Methods

The interfacial shear strength (IFSS) adhesion measurement of the aligned continuous fiber composite was done using a microindentation test. The microindentation tests were performed on a commercially available Interfacial Testing System (ITS) developed by Dow Chemical Co. Inc. [30]. This fully automated instrument is designed to test real composite specimens. The ITS is constructed on a Mitutoyo optical microscope. A diamond-tipped, hemispherical indenter mounted on the objective lens is used to indent single fibers in the composite specimens. The microindentation testing can be done by an automatic or semiautomatic debond technique. Initiation of fiber debond is sensed by a load cell attached to the sample holder. The motion of the sample holder is controlled using a precision-controlled, motorized

stage with three degrees of freedom. A television camera and monitor are used to observe the debonding. The force required to debond the fiber is input to a computer program that utilizes a closed-form algorithm derived by Mandell et al. [31] based on a least-squares fit of a set of solutions using finite element analysis. The interfacial shear strength (IFSS) was calculated based on the load at debonding. The generalized Eq. (1) is used to calculate the IFSS:

$$\tau = \sigma \left\{ A^* \left(\frac{G_m}{E_f} \right)^{0.5} + B^* \text{Ln} \left(\frac{T_m}{D} \right) + C \right\}, \quad (1)$$

where τ is the IFSS, σ the axial stress in the fiber at debond, G_m the shear modulus of the matrix, E_f the axial tensile modulus of the fiber, T_m the distance of the nearest neighbor of the tested fiber, and D the diameter of the tested fiber. The theory and the analysis of the various factors affecting the microindentation test can be found in Drzal and Herrera-Franco [32].

The transverse tensile test of the composite specimens was done on an Applied Test Systems (Butler, PA), Series 1600 Universal Testing Machine, with a 1000 lb (455 kg) load cell with an accuracy of 0.5%. The tests were done at a crosshead speed of 0.05 inches/minute (~ 1.3 mm/minute). The crosshead displacement was used to determine the “engineering” strain on the composite specimen.

The fractured transverse tensile test specimens were imaged using an Electroscan 2020 environmental scanning electron microscope with a 1.0 mm bore gaseous secondary electron detector at an accelerating voltage of 20 KeV in water vapor at a pressure of 3 torr and relative humidity of 10% to 30%. The images were stored as 1024 \times 1024 pixel TIFF files.

RESULTS AND DISCUSSION

Interfacial Adhesion in Low Molecular Weight Grafted Composites

The interfacial adhesion of the BPA-PC grafted carbon fiber composites is given in Table 1 and Figure 4. The interfacial adhesion differences between the ungrafted and the BPA-PC grafted fibers show that there is around 25% improvement in the level of adhesion for the 20% surface-treated IM7 fibers, from 21 MPa to 26 MPa. There is a much greater improvement in the level of adhesion in the 100% to 400% surface-treated fibers, with IFSS values for the grafted fibers ranging from 42.5 MPa to 49.2 MPa, an improvement of 60% to 80%

TABLE 1 The Interfacial Adhesion of the Ungrafted and BPA-PC-grafted, IM7 Series Carbon Fibers in Bisphenol-A Polycarbonate Matrix

Degree of fiber surface treatment %	Ungrafted (MPa)	BPA-PC grafted (MPa)
20	21.0 ± 2.63	25.9 ± 4.07
100	27.0 ± 1.94	49.2 ± 5.92
200	26.5 ± 2.65	42.5 ± 2.21
400	28.6 ± 3.15	47.3 ± 4.15

over the ungrafted surface. The lower level of improvement in the interfacial adhesion due to polymer grafting onto the 20% surface-treated fiber can be attributed to the lower number of grafted chains. Taking the statistical variation in the IFSS into consideration, we observe that there is no change in the level of adhesion with changing surface treatment at 100% and above. Based on the theory of cohesive zone failure proposed by Xu *et al.* [9], the results indicate that the areal density of the grafted chains must be sufficiently large for large-scale plastic deformation or crazing to be the dominant failure mode in these low molecular weight BPA-PC grafted carbon fiber composites. The surface area ratio increase and the mean roughness of a similar set of fibers, IM6 series carbon fibers shown in Figure 5 [23], indicate a nonmonotonous increase in the surface area with surface treatment. A similar trend was observed in the amount of active surface area on the IM7 series fibers, based on the volume of the methane evolved during the hydrogenation reaction [23].

Table 2 shows that the volume of methane evolved from IM7 series carbon fibers with different degrees of surface treatment. Since methane is evolved from the reaction of the carbon atoms on the edge planes with hydrogen, the volume of methane evolved can be directly correlated to the total active surface area of the fiber. If the nominal surface concentration of carbon on the surface of the fibers is taken to be about 10^{15} atoms/cm², and since it is well established by BET measurements that the nominal surface area of the commercially available PAN-based carbon fibers is around 0.5 m²/gram [26], then the total number of surface carbon atoms on these fibers would around 5×10^{18} atoms/gram, or about 7 μ moles/gram. Based on the amount of methane evolved during the hydrogenation, the active surface area ranges between 12% to 15% of the total surface area.

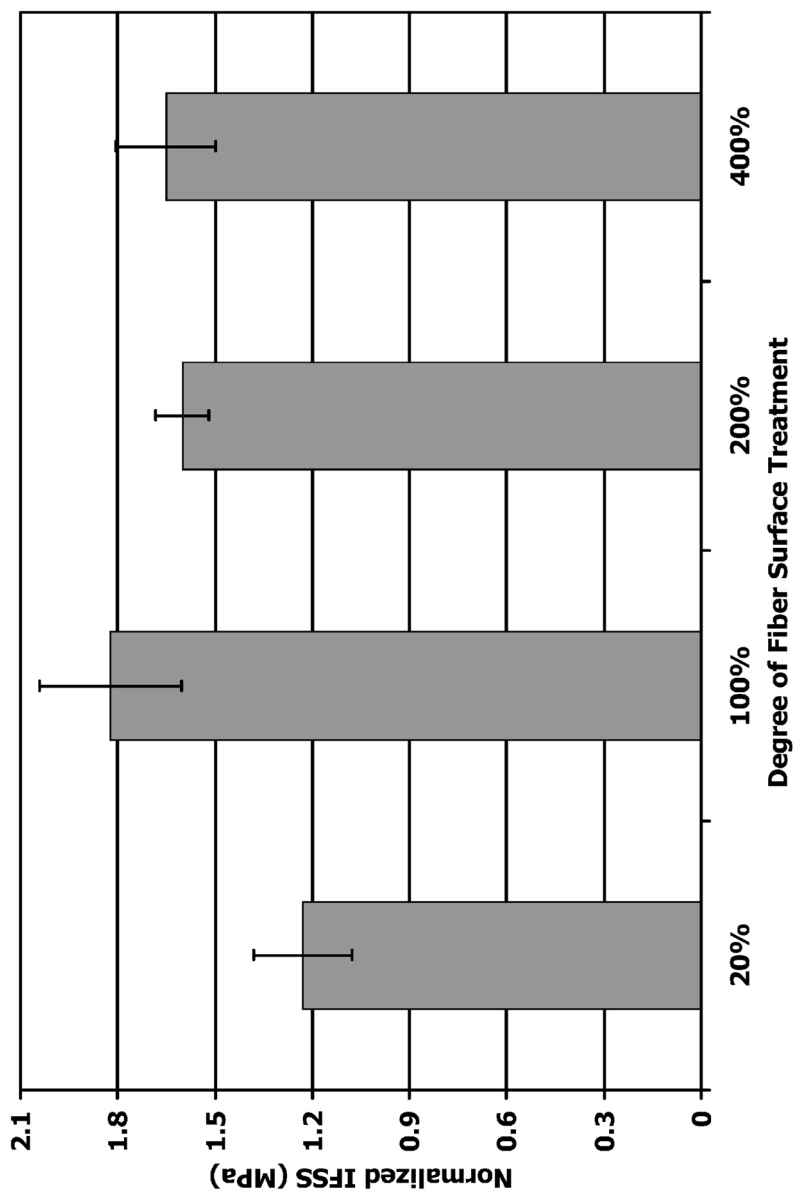


FIGURE 4 Normalized interfacial shear strength in the BPA-PC grafted carbon fiber-polycarbonate composites. The IFSS has been normalized with respect to the IFSS of ungrafted polycarbonate composite made with IM7 100% ST fibers.

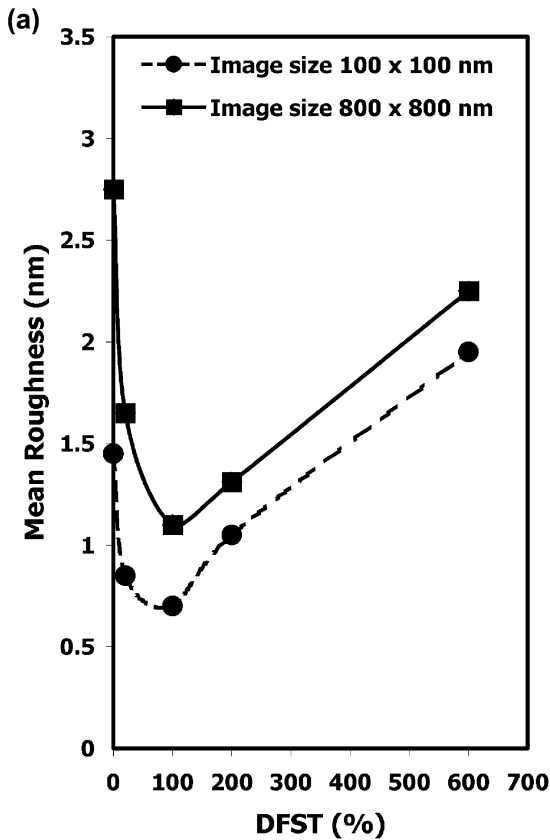


FIGURE 5 The surface roughness and surface area ratio increase with the degree of fiber surface treatment (DFST) obtained from the STM analysis of an IM6 series carbon fiber [25]. (*Continued.*)

This result indicates that even though the surface area of the fiber increases with increasing degree of fiber surface treatment, the active surface area of the fiber remains a constant fraction of the total surface area. The probability of all the surface-active sites initiating polymerization is small. The carbon fiber surface is composed of turbostratic layers of graphitic crystallites ranging in size from 2.5 to 8.0 nm. The basal structure of the graphitic crystallite consists of carbon surrounded by 6 other carbon atoms, and each of the carbon atoms is bonded to 3 other carbon atoms through sp^2 hybridized orbitals. This makes the bonds highly stable and not susceptible to attack by most reagents. In contrast, the edges of these crystallites

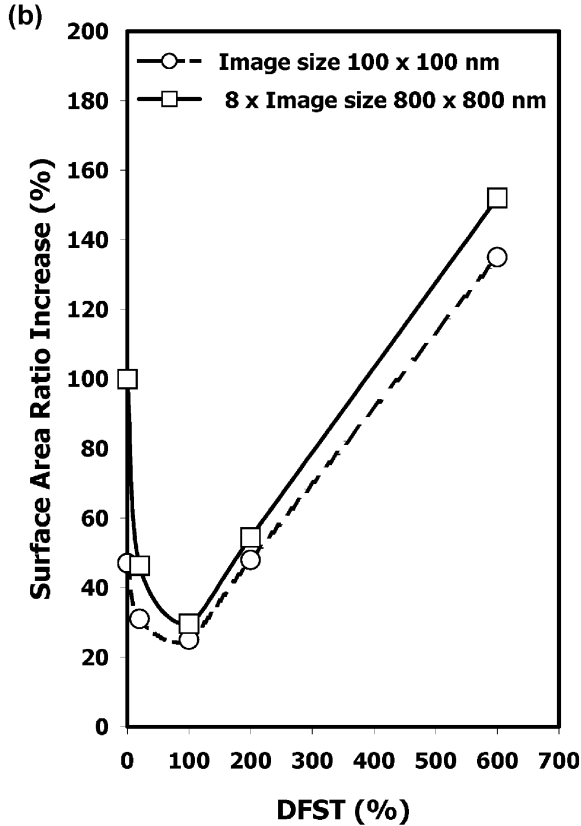


FIGURE 5 (Continued.)

TABLE 2 The Amount of Methane Evolved during the Hydrogenation of IM7 Series Carbon Fibers and Equivalent Values of the Active Surface Area

Degree of fiber surface treatment (%)	Volume of methane evolved ($\mu\text{L}/\text{gram}$)	Moles of methane evolved	Equivalent active surface area (m^2/gram)	Total surface area* (m^2/gram)
20	31.2	1.4×10^{-6}	0.083	0.6
100	29.1	1.2×10^{-6}	0.072	0.5
200	33.2	1.5×10^{-6}	0.090	0.6
400	43.8	2.0×10^{-6}	0.12	0.8

*Total surface area based on the nominal surface area of $0.5 \text{ m}^2/\text{gram}$ for IM7 100% surface-treated fiber and the surface area increase with the degree of fiber surface treatment measured by STM.

contain unsaturated carbon atoms amenable to functionalization. These edge sites on the surface of the fiber are the active sites for metalation and grafting of the polymer chains.

The ability of a surface site to initiate polymerization depends on its ability to be converted to an anion as well as the initial concentration of the reactant monomers and oligomers. Even if the amount of grafting were proportional to the amount of active surface area, the overall surface areal density of the grafted chains would be relatively small. Further, as shown in Figures 6 and 7, the surface topography of the carbon fiber is very different from an ideal surface. The basal planes consisting entirely of carbon-carbon bonds are highly dispersive in character and most polymer chains do not have any affinity to adsorb on them strongly, while the edge planes of the graphitic crystallites contain the active sites. As can be seen in the STM micrograph (Figure 5), the edge planes are very close to each other. Due to this proximity of the active sites the level of grafting would be dependent on the backbone structure and the presence of any sterically hindering groups on the reacting oligomer. The initiation of polymerization at any site can hinder the initiation in the surrounding sites that are separated from the initiated site by less than the steric volume of the grafted oligomer. Since only 12% to 15% of the total surface area of the fiber can actively initiate grafting there is a large amount of non-reactive basal plane separating the growing chains on either side of the graphitic crystallite, so at even the highest possible concentration of the grafted chains on the surface there would be a sufficient amount of free basal surface for the grafted chains to bend over and coil. This unique configuration of the active sites and the ability of the grafted chain to have brushlike density but mushroom-like conformation allows for an optimum amount of entanglement with the bulk matrix. An increase in the grafting density would, however, allow efficient stress transfer and formation of crazes in the grafted layer, resulting in large plastic deformation during the chain pull-out process.

Interfacial Adhesion in High Molecular Weight Grafted Composites

The interfacial adhesion of the PMMA-grafted chains is shown in Table 3 and Figure 8. The level of adhesion in these long-chain grafted composites also shows a large increase over the ungrafted composites. The level of improvement in adhesion ranges from 25% to 70% with increasing degree of fiber surface-treatment. For the IM7 20% surface-treated fiber, the increase in the level of adhesion over the ungrafted composites is relatively lower—at 33% for the oxidized fibers compared

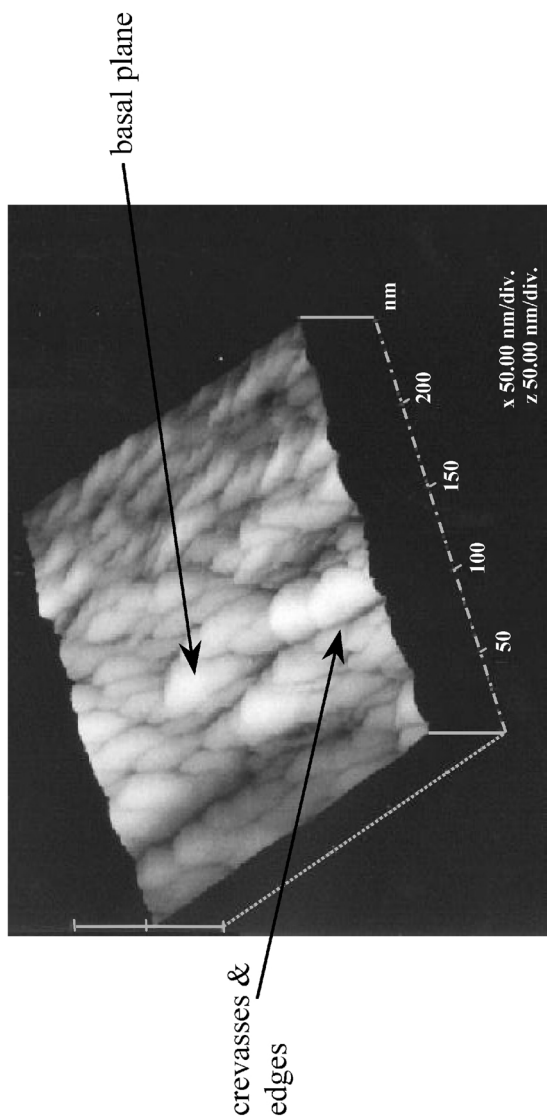


FIGURE 6 The scanning tunneling microscopy (STM) image of the IM6 carbon fiber showing the unique topography of these fibers for the grafting studies.

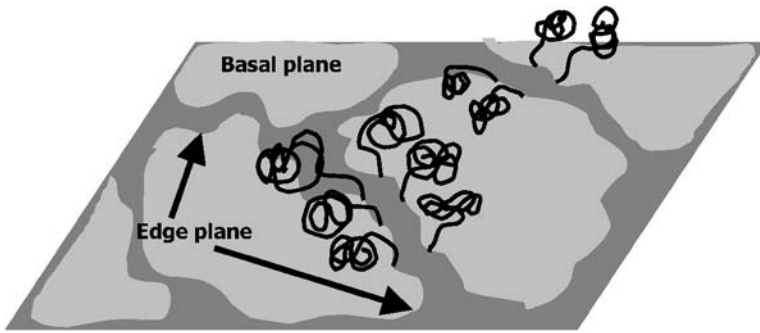


FIGURE 7 A schematic diagram of the carbon fiber surface showing the basal plane and the likely location of the grafted chains at the edges of the graphite crystallites.

with an increase of 60% for the hydrogen-passivated fibers. This further confirms that the amount of electrolytic oxidative surface treatment for the 20% surface-treated fiber is not sufficient to remove all of the weak polyaromatic boundary layer present on the fiber surface. Hydrogenation of the fiber up to 1000°C removes any remaining weak boundary layer prior to metalation, reducing the cohesive failure in the fiber and thereby improving the IFSS. As observed earlier in the BPA-PC-grafted fibers, the improvement in the interfacial adhesion is higher for the 100% to 400% surface-treated fibers, but this increase is relatively constant, ranging from 50% to 60% over the IFSS of the corresponding ungrafted composites fabricated from fibers with same degree of surface treatment. The large increase in the interfacial adhesion between the polymer-grafted fibers and the bulk matrix

TABLE 3 The Interfacial Adhesion of the PMMA-Grafted IM7 Series Carbon Fiber/BPA-PC Matrix Composites Containing Oxidized and Hydrogen-Passivated Fibers

Degree of fiber surface treatment (%)	Oxidative surface treated (ungrafted) (MPa)	Oxidative surface treated (MPa)	Hydrogen passivated (MPa)
20	21.0 ± 2.63	28.0 ± 3.42	33.2 ± 3.63
100	27.0 ± 1.94	40.3 ± 5.65	34.4 ± 2.64
200	26.5 ± 2.65	44.8 ± 3.88	47.3 ± 4.02
400	28.6 ± 3.15	45.2 ± 5.69	47.6 ± 6.77

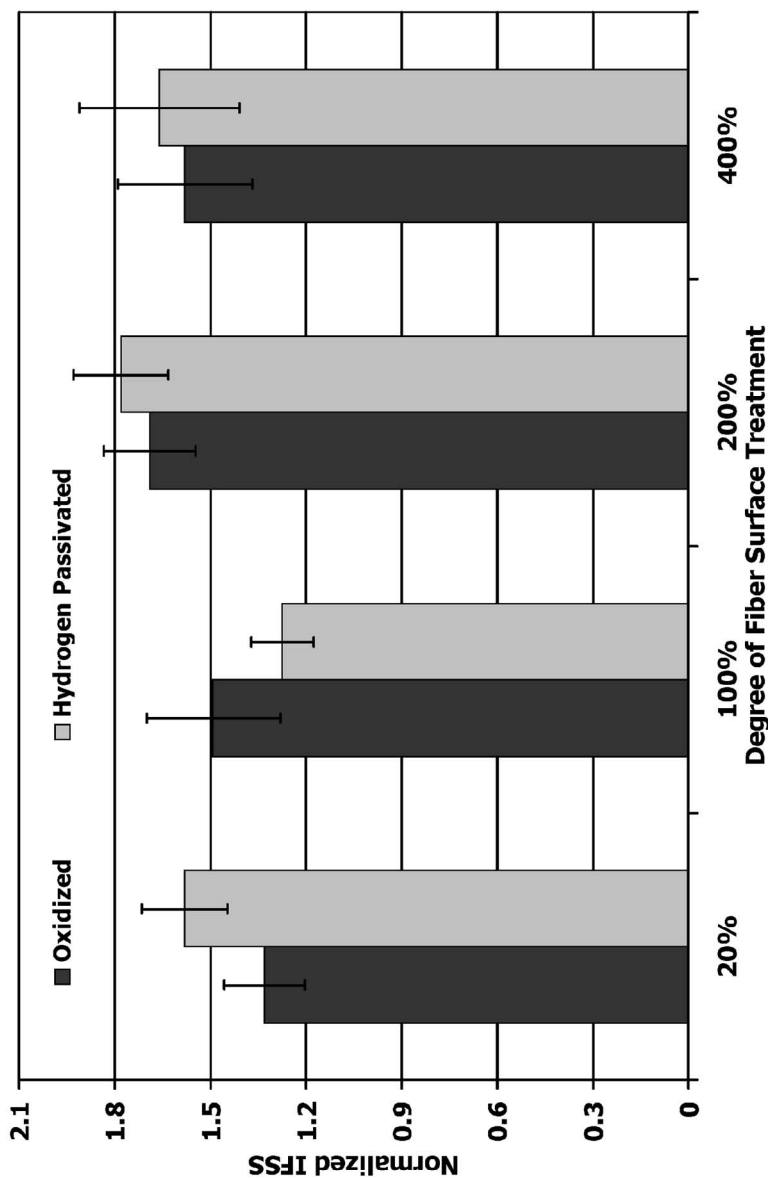


FIGURE 8 Interfacial shear strength in the PMMA grafted carbon fiber-polycarbonate composites. The IFSS has been normalized with respect to the IFSS of ungrafted polycarbonate composite made with IM7 100% ST fibers.

indicates that grafting polymer chains to the surface is indeed a useful method to improve composite mechanical properties. These results indicate that the improvement in the interfacial adhesion in these composites is independent of the degree of surface treatment.

Since PMMA grafted onto the carbon fiber surface has a relatively higher molecular weight than the bulk polycarbonate matrix, the debonding at the surface would be occurring by chain scission. TGA analysis of the grafted surface indicates that the amount of polymer grafted on the surface ranges from 0.7% to 2.5% by weight [11], while the BPA-PC grafted onto the surface ranged from 1.3% to 2.1%. This relatively similar amount of grafting for two polymers having very different chain lengths indicates that the surface areal density of PMMA grafted onto the surface is much lower than for the BPA-PC graft. But the level of improvement in the interfacial adhesion is comparable for these two different molecular weight grafted chains, as shown in Figure 9. The interphase deformation map shown in Figure 1 can explain these observations. In the case of chain pull out, the surface areal density, Σ , of the grafted chains has to be large ($\gg \Sigma_C$) for the large-scale plastic deformation stresses, σ_{craze} , to become predominant. For chain scission, if the surface areal density is higher than the critical density, Σ_C , the normal stresses on the interface would initiate crazing.

The results of the adhesion tests indicate that the interfacial adhesion is independent of the chain length of the grafted layer. The level of adhesion was also observed to be independent of the degree of surface treatment for the different chain lengths of the grafted polymers, indicating that the surface areal density in both cases must be sufficiently large for the large-scale plastic deformation and crazing to dominate the failure at the interface. The interfacial shear strength improvements in the grafted composites over the ungrafted composites, as shown in Figure 10 for both the electrolytically oxidized and subsequent hydrogen-passivated surfaces, indicates that the formation of a strongly bonded but impenetrable boundary at the interface due to polymer grafting is a useful technique for achieving improved composite mechanical properties. Further, the grafting of polymers onto the reinforcing fibers not only improves the mechanical properties of the composite but also improves its ability to withstand environmental effects such as attack by moisture.

Further evidence of the effectiveness of grafting is shown by the transverse tensile tests of the model composites in Table 4 and Figure 11. While the interfacial shear strength and transverse tests produce a different state of stress on the fiber-matrix interface, the trends of increasing adhesion with surface treatment should be the same. These

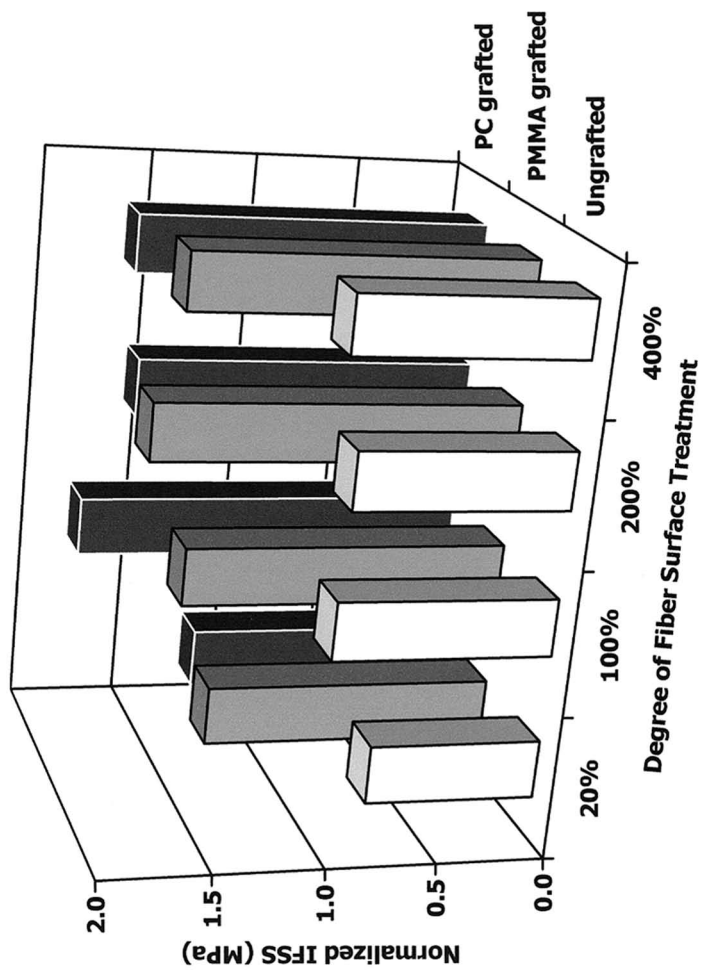


FIGURE 9 Comparison of the interfacial adhesion between composites having ungrafted and grafted chains of different molecular weight.

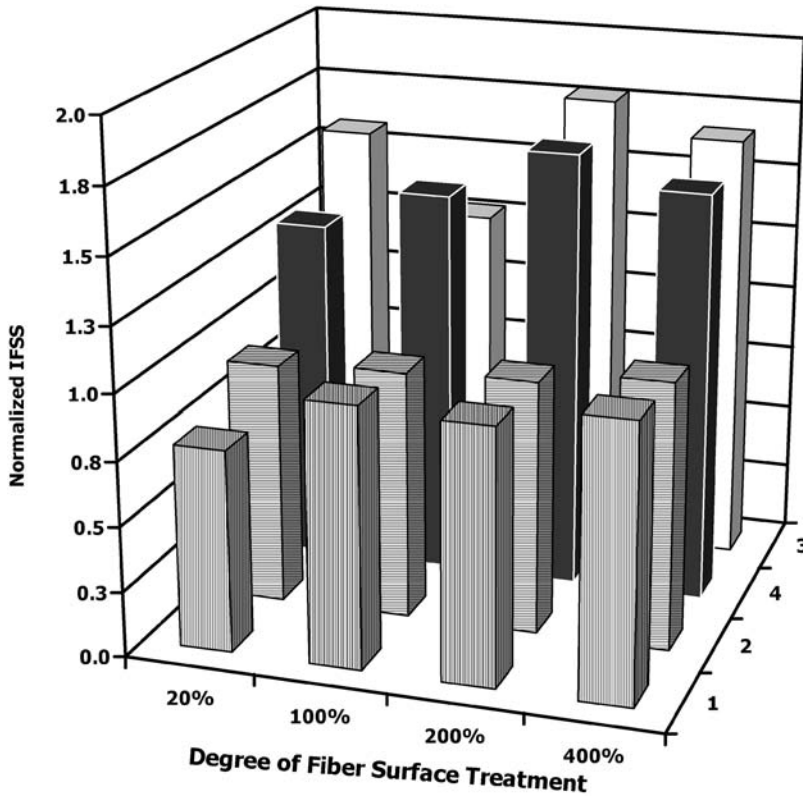


FIGURE 10 Comparison between the interfacial adhesion in the ungrafted and polymer-grafted carbon fiber composites, where (1) is the oxidized fiber ungrafted composite, (2) is the hydrogenated ungrafted composite, (3) is the oxidized and PMMA grafted, and (4) is the hydrogenated fiber with PMMA grafted onto it.

TABLE 4 The Transverse Tensile Strength of the Ungrafted and BPA-PC-Grafted Carbon Fibers in Bisphenol-A Polycarbonate Matrix

Degree of fiber surface treatment (%)	Ungrafted (MPa)	BPA-PC grafted (MPa)
20	47.19 ± 1.93	49.31 ± 2.42
100	44.59 ± 2.13	51.18 ± 1.09
200	48.67 ± 6.31	54.33 ± 3.07
400	54.26 ± 1.31	57.12 ± 5.60

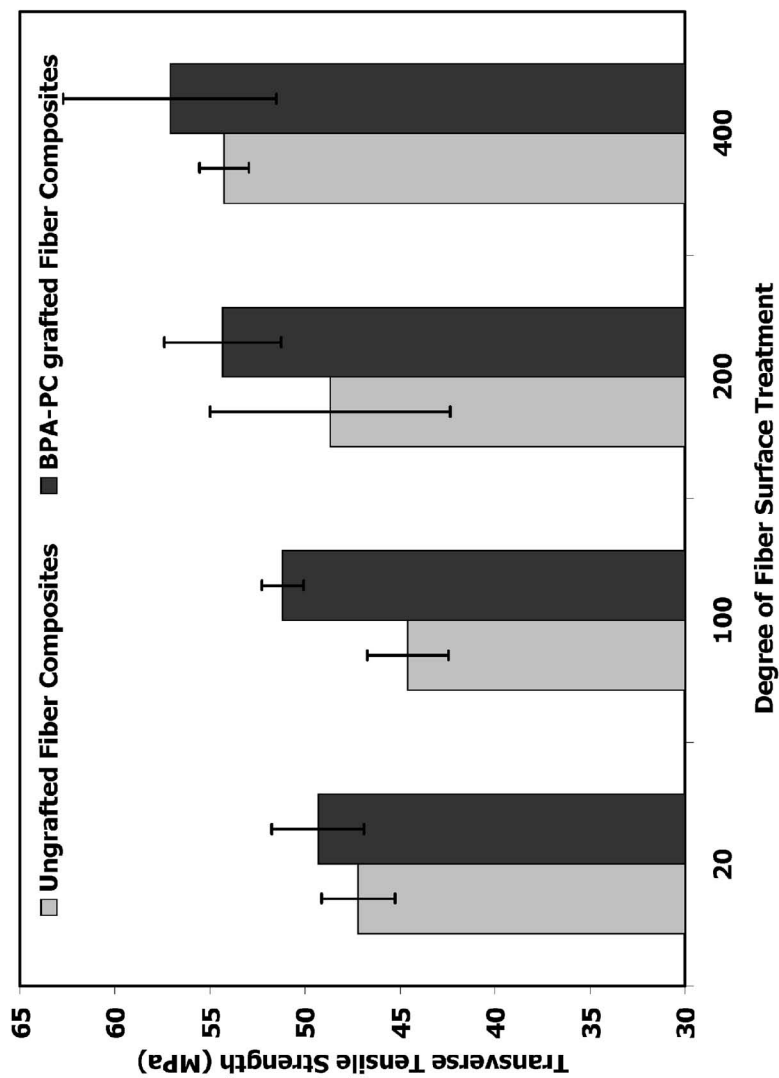


FIGURE 11 The transverse tensile test results of PC grafted and ungrafted composite, showing the difference in the transverse strength values as a function of carbon fiber surface treatment.

transverse results do indicate a higher tensile strength for the PC-grafted composites compared with the ungrafted composites for all degrees of fiber surface treatment. Further, these grafted fiber composites failed by a different mechanism (*i.e.*, failure occurred in the composite), whereas the ungrafted composites generally failed in the composite followed by necking and failure of the polycarbonate backing sheet. This indicates that the strain energy released from the ungrafted fiber composite failure is not sufficient to rupture the polycarbonate backing, while all of the grafted composites failed by rupture along with breaking of the polycarbonate backing sheet without any necking. This indicates that the energy released during the failure of the PC-grafted specimens is higher than the tensile toughness of the polycarbonate.

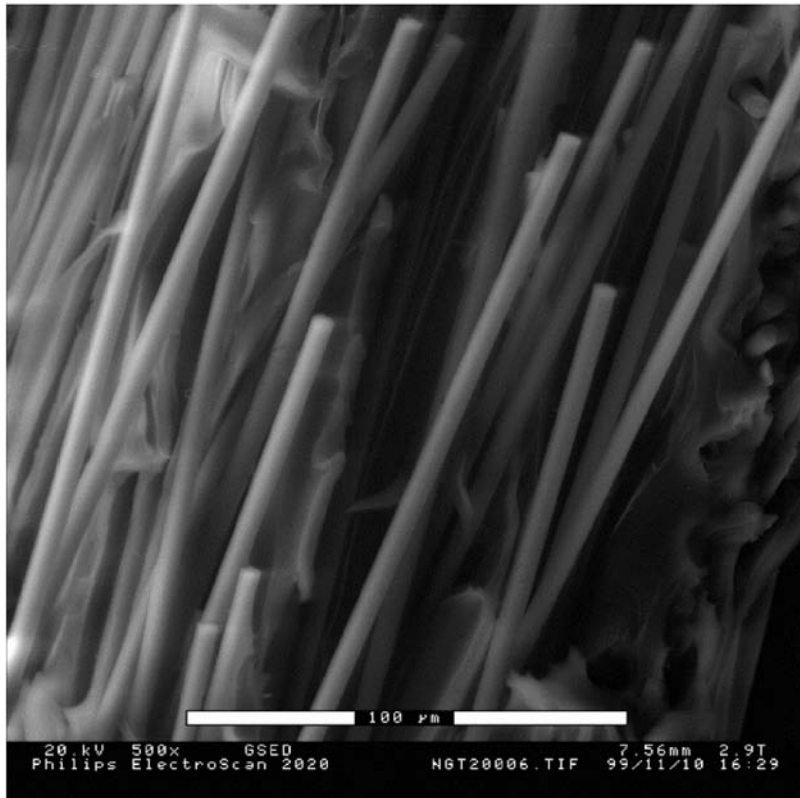


FIGURE 12 ESEM image of the fracture surface of an ungrafted polymer composite.

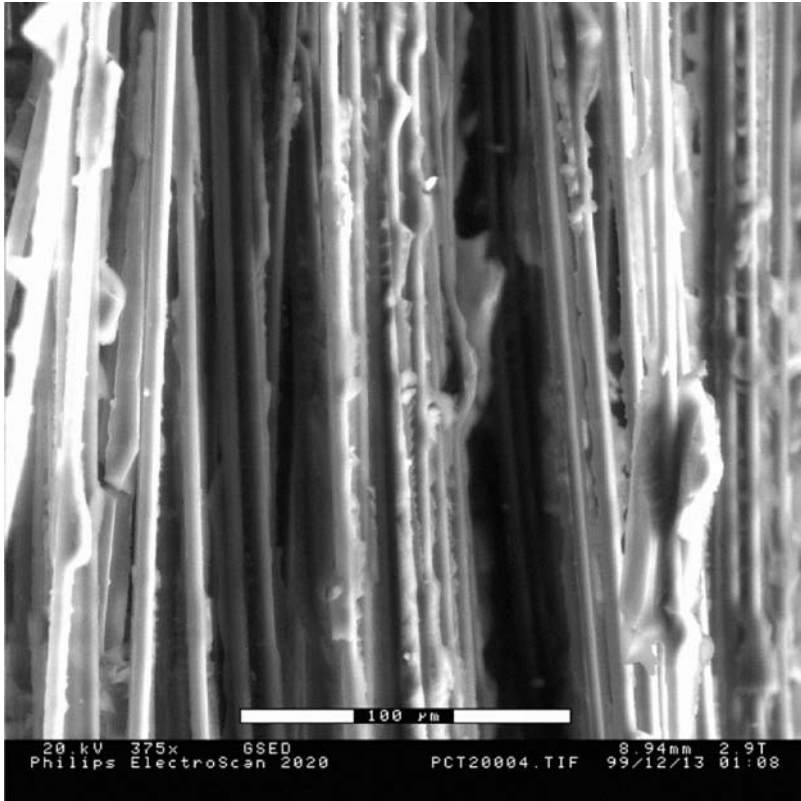


FIGURE 13 ESEM image of the transverse tensile fracture surface of a BPA-PC-grafted polymer composite.

The ESEM micrographs of ungrafted and PC-grafted specimens are shown in Figures 12 and 13, respectively. It can be clearly seen that in the ungrafted composites the failure in the composite is adhesive in nature, *i.e.*, the composites failed at the interface between the matrix and the fibers. Bare fibers are clearly visible on the fracture surface. The fracture surface of the PC-grafted composites shown in Figure 13 is predominantly cohesive in the matrix. All fibers are covered with matrix. The results from the electron microscopy shows that with the grafting of polymer chains the maximum possible level of adhesion can be achieved.

CONCLUSIONS

The interfacial adhesion between a thermoplastic polycarbonate matrix and a carbon fiber having polymer grafted onto its surface was experimentally investigated. Grafting low molecular weight BPA-PC chains and high molecular weight PMMA chains on both the electrolytically oxidized and hydrogen-passivated surfaces of the IM7 series, fibers with different degrees of surface treatment show improvement in the interfacial adhesion ranging from 20% to 80% over corresponding ungrafted fiber composites. It was also seen that the level of improvement in the interfacial adhesion is independent of the chain length above a critical length and density of grafting. The increase in level of adhesion is not dependent on the degree of chemical surface treatment for carbon fibers with treatment above 100% for the entire set of fibers with different grafted chain lengths, indicating that the surface areal density of the grafting is sufficiently large so that large-scale plastic deformation and crazing predominates the failure at the interface. The surface structure of the carbon fiber also allows good entanglement of the grafted polymer with the bulk polymer, facilitating the development of strength and toughness in the polymer-grafted carbon fiber composites. The fracture surface of grafted-fiber composites also show failure to be predominantly cohesive in the matrix, indicating that the maximum possible level of adhesion in thermoplastic composites was achieved by polymer grafting.

REFERENCES

- [1] Raghavendran, V., Drzal, L. T., and Askeland, P. J., *J. Adhes. Sci. Technol.*, **16**, 1283–1306 (2002).
- [2] Raghavendran, V., Waterbury, M. C., Rao, V. and Drzal, L. T., *J. Adhes. Sci. Technol.*, **11**(12), 1501–1512 (1997).
- [3] deGennes, P. G., *J. Phys. (Paris)*, **37**, 1443–1448 (1976).
- [4] Alexander, S., *J. Phys. (Paris)*, **38**, 983–987 (1977).
- [5] Fleer, G. J., Cohen Stuart, M. A., Scheutjens, J. M. H. M., Cosgrove, T. and Vincent, B., *Polymers at Interfaces* (Chapman & Hall, New York and London, 1993).
- [6] DiBenedetto, A. T., Huang, S. J., Birch, D., Gomez, J. and Lee, W. C., *Compos. Struc.*, **27**, 73–82 (1994).
- [7] Chou, C. T. and Penn, L. S., *J. Adhesion*, **36**, 125–137 (1991).
- [8] Kramer, E., Norton, L. J., Smigolova, V., Pralle, M. U., Hubenko, A., Dai, K. H., Hahn, S., Berglund, C. and Dekoven, B., *Macromolecules*, **28**(6) 1999–2008 (1995).
- [9] Xu, D. B., Hui, C. Y., Kramer, E. J. and Creton, C., *Mech. Mater.*, **11**, 257–268 (1991).
- [10] Leger, L., Raphael, E., and Hervet, H., *Adv. Polym. Sci.*, **138**, 185–225 (1999).
- [11] Raghavendran, V. and Drzal, L. T., *Comp. Infr.*, 1–24 (2002).
- [12] Brandrup, J. and Immergut, E. H., Eds., *Polymer Handbook* (Wiley, New York, 1989).

- [13] David, D. J., *MATPROP, The Miscibility Parameter Estimation Software*, Ver. **2.3**, Copyright: S. F. Technologies (1993).
- [14] Kim, C. K. and Paul, D. R., *Macromolecules*, **25**, 3097–3105 (1992).
- [15] Kyu, T. and Saldanha, J. M., *Macromolecules*, **21**, 1021–1026 (1988).
- [16] Kyu, T., Ko, C. C. and Smith, S. D., *J. Polym. Sci., Part B: Polym. Phys.*, **33**, 517–525 (1995).
- [17] Debier, D., Devaux, J. and Legras, R., *J. Polym. Sci., Part A: Polym. Chem.*, **33**, 407–414 (1995).
- [18] Lai, J. Y., Huang, S. J., Huang, S. L. and Shyu, S. S., *Sep. Sci. Technol.*, **30**, 461–476 (1995).
- [19] Guerrero, A. R. and Ramirez, J. C., *Polym. Bull.*, **33**, 541–548 (1994).
- [20] Koo, K. K., Inoue, T. and Myasaka, K., *Polym. Eng. Sci.*, **27**, 741–746 (1985).
- [21] Chiou, J. S., Barlow, J. W. and Paul, D. R., *J. Polym. Sci., Part B: Polym. Phys.*, **25**, 1459–1471 (1987).
- [22] Montaudo, G., Puglisi, C. and Samperi, F., *Macromolecules*, **31**, 650–661 (1998).
- [23] Raghavendran, V., Ph.D. Dissertation, Department of Chemical Engineering, Michigan State University (1999).
- [24] Raghavendran, V. and Drzal, L. T., *J. Thermopl. Comp. Mater.*, submitted for publication (2001).
- [25] Drzal, L., Sugiura, N. and Hook, D. J., *Compos. Interfaces*, **4**, 337–354 (1997).
- [26] Hoffman, W. P., Hurley, W. C., Owen, T. W. and Phan, H. T., *J. Mater. Sci.*, **26**, 4545 (1991).
- [27] Guigon, M., Oberlin, A. and Desarmot, G., *Fibre Sci. Technol.*, **20**(3), 177–198 (1984).
- [28] Raghavendran, V., M.S. Thesis, Department of Chemical Engineering, Michigan State University (1994).
- [29] Waterbury, M. C. and Drzal, L. T., *Controlled Interphases in Composite Materials*, H. Ishida, Ed., Elsevier Science, The Netherlands, 731 (1990).
- [30] Tse, M. K., U.S. Patent 4,662,228, assigned to Dow Chemical Co., Inc. (1987).
- [31] Grande, D. H., Mandell, J. F. and Hong, K. C. C., *J. Mater. Sci.*, **23**, 311–328 (1988).
- [32] Drzal, L. T. and Herrera-Franco, P. J., In: *Engineered Materials Handbook*, **3** 391–405 (ASM International, Materials Park, OH, 1991).